The Journal of Veterinary Medical Science

FULL PAPER

Anatomy

The effects of astaxanthin on liver histopathology and expression of superoxide dismutase in rat aflatoxicosis

Poempool MONMEESIL[1)], Wirasak FUNGFUANG[2)], Phitsanu TULAYAKUL[3)] and Urai PONGCHAIRERK[1)]*

[1)]Department of Anatomy, Faculty of Veterinary Medicine, Kasetsart University, 50 Ngamwongwan Road, Ladyao, Jatuchak, Bangkok 10900, Thailand
[2)]Department of Zoology, Faculty of Science, Kasetsart University, 50 Ngamwongwan Road, Ladyao, Jatuchak, Bangkok 10900, Thailand
[3)]Department of Veterinary Public Health, Faculty of Veterinary Medicine, Kasetsart University, Malaiman Road, Kamphaeng Saen, Nakhon Pathom 73140, Thailand

ABSTRACT. The metabolism of aflatoxin B_1 (AFB_1) generates reactive oxygen species (ROS) that destroys hepatocytes. Meanwhile, astaxanthin (AX) is known to have stronger antioxidative activity than other carotenoids. This study aimed to investigate hepatoprotective role of AX from AFB_1-induced toxicity in rat by histopathological study and immunohistochemistry of Cu/Zn-SOD (SOD1) which acts as the first enzyme in antioxidative reaction against cell injury from ROS. Twenty Wistar rats were randomly divided into 4 groups. The control and AFB_1 groups were gavaged by water for 7 days followed by a single DMSO and 1 mg/kg AFB_1, respectively. The AXL+ AFB_1 and AXH+ AFB_1 groups were given of 5 mg/kg and 100 mg/kg AX for 7 days before 1 mg/kg AFB_1 administration. The result showed significantly elevated liver weight per 100 g body weight in AFB_1 group. The histopathological finding revealed vacuolar degeneration, necrosis, megalocytosis and binucleation of hepatocytes with bile duct hyperplasia in AFB_1 group. The severities of pathological changes were sequentially reduced in AXL+AFB_1 and AXH+AFB_1 groups. Most rats in AXH+AFB_1 group owned hypertrophic hepatocytes and atypical proliferation of cholangiocytes which are adaptive responses to severe hepatocyte damage. The SOD1 expression was also significantly higher in AXH+AFB_1 group than solely treated AFB_1 and AXL+AFB_1 groups. In conclusion, AX alleviated AFB_1-induced liver damage in rat by stimulating SOD1 expression and transdifferentiation of cholangiocytes in dose dependent manner.

KEY WORDS: aflatoxin B_1, astaxanthin, histopathology, immunohistochemistry, superoxide dismutase

J. Vet. Med. Sci.
81(8): 1162–1172, 2019
doi: 10.1292/jvms.18-0690

Received: 20 November 2018
Accepted: 19 June 2019
Advanced Epub: 3 July 2019

Aflatoxin is a group of mycotoxins which are produced by *Aspergillus* spp., especially *A. flavus*, *A. parasiticus* and *A. nomius* [18]. This health hazardous toxin can be found as a contaminant in agricultural commodities during cultivation, harvesting, transport and storage in various regions with hot and humid climates [2, 18, 47]. Aflatoxin B_1 (AFB_1) is the most potent hepatotoxic agent which causes histopathological changes of liver such as necrosis, vacuolar degeneration, fatty changes, megalocytosis and binucleation of hepatocyte. Furthermore, bile duct hyperplasia and periportal fibrosis are observed [1, 2, 48, 49]. During AFB_1 metabolism activated by cytochrome P450, the reactive oxygen species (ROS), such as superoxide ion (O_2^-) and hydrogen peroxide (H_2O_2), are produced excessively leading to oxidative stress that could be eradicated by antioxidants [27, 44]. However, the overwhelming oxidative stress beyond an ability of antioxidants to handle results in damage of critical macromolecules (lipid, DNA and protein) and loss of biological functions such as calcium influx, membrane leakage and consequently affected DNA stability that leads to cancer [21, 25, 41]. The oxidative damage can be protected by enzymatic antioxidants, including superoxide dismutase (SOD), glutathione peroxidase (GPX) and catalase (CAT), and non-enzymatic mechanisms by low molecular mass compounds such as glutathione, ascorbic acid, α-tocopherol and carotenoids [15]. The function of enzymatic antioxidants is to prevent the ROS from attacking other essential proteins in the cell by converting oxidative products into non dangerous molecules by multi-step processes, while the activity of non-enzymatic antioxidants is to interrupt free radical chain reactions and neutralize the ROS in a process called radical scavenging [31]. One of the key anti-oxidative enzymes, SODs, is a family of enzymes that are important for the biological defense of cell injuries mediated through oxygen free radicals. The three main SOD isoforms have been identified in mammalian cells with different localization: the cytosolic Cu/Zn-SOD (SOD1), mitochondrial Mn-SOD (SOD2) and extracellular Cu/Zn-SOD

*Correspondence to: Pongchairerk, U.: fveturp@ku.ac.th, au_urai@yahoo.com

(SOD3). They detoxify superoxide ion and change into hydrogen peroxide which is inactivated by CAT into oxygen and water which are not harmful for cells. In hepatocyte, SOD1 expression is in the cytoplasm, followed by inside the nucleus. Its distribution was clarified to overlap with the site of superoxide production. High concentration of SOD1 was found in lysosome by nonselective autophagy since it is resistant to protease digestion. Surprisingly, the endoplasmic reticulum (ER) does not contain remarkable concentrations of SOD1 because the production of superoxide is on the cytoplasmic side which towards the surrounding cytoplasm whereas it is very low inside the ER cisternae. In mitochondria, the superoxide is formed by electron released from electron transport chain, but SOD2 plays major protective role in this part instead of SOD1 [6, 9].

Astaxanthin (AX) (3,3′-dihydroxy-β, β-carotene-4,4′-dione) is a red carotenoid pigment found in microorganisms such as the green algae *Haematococcus pluvialis* [36], the red yeast *Phaffia rhodozyma* [7], and in many marine animals [43]. It has been used as a feed supplement to promote growth, egg quality, muscle and yolk pigmentation, immune system and antioxidant capacity in livestock, especially aquatic animals and poultry [35, 43]. AX has been reported as a powerful non-enzymatic antioxidant for scavenging variety of free radicals. Its antioxidative activity is 10 times stronger than zeaxanthin, lutein, tunaxanthin, canthaxanthin and β-carotene, and 100 times greater than α-tocopherol [26, 29]. AX can protect acute CCl_4 induced liver damage by inhibiting lipid peroxidation and increasing antioxidative mechanism by stimulating glutathione and SOD activities [20]. It prevents liver fibrosis by suppressing multiple profibrogenic factors in mice [39]. Moreover, AX also has anti-inflammatory activity by suppressing the level of NF-kB which regulates the production of inflammatory mediators [22]. Although AX has been widely studied for its hepatoprotective property, the investigation of AX activity on liver protection prior to an acute AFB_1 administration in rat has never been studied. In present study, we focused on histopathological changes and immunohistochemistry of SOD1 in AFB_1 intoxicated rats by comparing the two doses of 5 mg/kg or 100 mg/kg AX. Since the climate in Southeast Asia is suitable for the growth of *Aspergillus* spp., contamination of AFB_1 has been found frequently during the processes of human and animal food production. Therefore, this study will be beneficial for the preventive treatment of aflatoxicosis in human and animal in the future.

MATERIALS AND METHODS

Animals

A total of 20 male Wistar rats, 6-week-old, weighing 200–250 g were obtained from National Laboratory Animal Center (Nakhon Pathom, Thailand). All rats were acclimated at 22–25°C in 12 hr dark/light cycle and fed *ad libitum*. This study has been approved by the Institutional Animal Care and Use Committee of Kasetsart University, Thailand (ID# ACKU 61-VET-023).

Chemicals and preparation

Aflatoxin B_1 (Sigma-Aldrich, St. Louis, MO, U.S.A.) was dissolved in 50% (w/v) DMSO in distilled water to the final concentration of 1 mg/kg and fed for each rat [34]. AstaMax®10S (Guangzhou Juyuan Bio-Chem Co., Ltd., Guangzhou, China), 10% astaxanthin in calcium lignosulfonate, was daily prepared by dissolving in warm water as recommended by manufacturer into dosages of 5 mg/kg astaxanthin for low dose administration and 100 mg/kg astaxanthin for high dose administration [20]. Mouse monoclonal anti-SOD1 antibody, HRP-conjugated mouse IgG kappa chain binding protein (m-IgGκ BP-HRP), goat polyclonal anti-GAPDH antibody and HRP-conjugated donkey anti-goat IgG antibody were purchased from Santa Cruz Biotechnology, Inc., Dallas, TX, U.S.A. DAB peroxidase substrate kit was purchased from Vector Laboratories, Inc., Burlingame, CA, U.S.A.

Experimental design

The experimental animals were randomly divided into 4 groups of 5 rats: Control group (normal rats without AFB_1 intoxication and AX treatment), AFB_1 group (rats intoxicated by AFB_1), AXL+AFB_1 group (rats treated with low dose AX before AFB_1 intoxication) and AXH+AFB_1 group (rats treated with high dose AX before AFB_1 intoxication). The rats in control and AFB_1 groups were gavaged with 2 m*l* of distilled water for 7 days. At day 8, control rats were received 2 m*l* of 50% DMSO in distilled water whereas rats in AFB_1 group were received 1 mg/kg AFB_1. The rats in AXL+AFB_1 and AXH+AFB_1 groups were gavaged for 7 days with 5 mg/kg and 100 mg/kg astaxanthin, respectively. Then, both groups were also received 1 mg/kg AFB_1 at the 8th day. All rats were fed for the following 4 days and were euthanized at the 13th day by intraperitoneal injection with 60 mg/kg pentobarbital sodium and blood and liver tissue samples were then collected. During the experiment periods, the rats were weighed every day to observe weight gain.

Serum biochemistry

The blood samples were obtained from the experimental rats by cardiac puncture. The serum was separated and measured the levels of alanine aminotransferase (ALT) and aspartate aminotransferase (AST) by automated chemistry analyzer (Mindray® BS 380, Shenzhen Mindray Bio-Medical Electronics Co., Ltd., Shenzhen, China).

Histopathological examination

Entire liver was removed from each rat and weighed. The ratio of liver weight/100 g body weight (LW/100 g BW) was calculated. The liver tissue for histopathological study was cut and fixed in 10% neutral buffered formalin, dehydrated in graded alcohol series, cleared in xylene and embedded in paraffin. Tissue sectioning was done at 3 μm thickness and stained with hematoxylin and eosin (H&E). The histopathological observation was performed by Olympus® BX50 light microscope (Olympus Corp., Tokyo, Japan). The photographs of 40× magnification were taken and the cell numbers of hepatocyte alterations were

counted for 20 randomized areas of a square millimeter (mm^2).

Immunohistochemical staining

Paraffin sections of liver were deparaffinized, rehydrated and incubated in 10 mM citrate buffer (pH 6.0) at 95°C for antigen retrieval. Non-specific binding was blocked with 2% bovine serum albumin (BSA) in phosphate buffered saline (PBS). Mouse monoclonal anti-SOD1 antibody at a dilution of 1:500 was overnight incubated on liver tissue at 4°C. The tissues were washed with 0.05% Tween 20 in PBS (pH 7.4) and incubated with 3% hydrogen peroxide to inactivate endogenous peroxidase. The m-IgGκ BP-HRP at a dilution of 1:1,000 was applied and immunoreactivity of SOD1 was visualized by DAB peroxidase substrate kit. The tissue sections were then counterstained with hematoxylin and observed under light microscope.

Western blot analysis

The liver tissue was snap frozen by liquid nitrogen and kept in −80°C refrigerator. Total protein was extracted from homogenized tissue in RIPA buffer containing protease inhibitor cocktail (Sigma-Aldrich). The supernatant was collected after centrifugation at 13,000 rpm for 20 min at 4°C. The protein concentrations of each sample were measured using Bio-Rad Protein Assay Dye Reagent Concentrate (Bio-Rad Laboratories, Inc., Hercules, CA, U.S.A.) and analyzed by Synergy H1 Hybrid Multi-Mode Microplate Reader with Gen5™ 2.0 Data Analysis Software (BioTek®, Winooski, VT, U.S.A.). The samples containing 25 μg of total protein were separated by 12.5% SDS-PAGE (100V for 90 min) and then transferred into nitrocellulose membrane by constant voltage of 100V for 1 hr at 4°C. The non-specific protein binding on the membrane was blocked with 5% non-fat milk in TBST and the membrane was then incubated with mouse monoclonal anti-SOD1 antibody (1:2,000 dilution). After washing with TBST, the membrane was incubated with m-IgGκ BP-HRP (1:5,000 dilution). The bands were detected by enhanced chemiluminescence (ECL) (Clarity™ Western ECL Substrate), visualized by ChemiDoc™ Imaging System and analyzed by Image Lab™ Software (version 6.0) (Bio-Rad Laboratories, Inc.). The same membrane was immersed in stripping buffer at 50°C for 30 min. The non-specific protein was blocked with 5% BSA and the membrane was reprobed with goat anti-GAPDH antibody (1:1,000 dilution) and HRP-conjugated anti-goat IgG antibody (1:5,000 dilution) as an internal control.

Data analysis

The average values of body weight gains, LW/100 g BW, liver enzyme parameters, numbers of hepatocyte alterations and normalized densitometry of SOD1/GAPDH from western blot analysis were presented as mean ± standard deviation (SD). The percentage of SOD1 stained area was measured by Image J (version 1.52a, National Institute of Health, Bethesda, MD, U.S.A.) from 5 different areas in each group and averaged to evaluate the density of SOD1 immunoreactivity. All data were analyzed by using Kruskal-Wallis test followed by Dunn's *post hoc* test. The R statistical software for Windows (version 3.5.0., R Core Team) was used to analyze statistical significance with an acceptable level at $P \leq 0.05$.

RESULTS

Effect of AX and AFB_1 on body weight

During the experimental period, none of the rats showed any signs of illness. All rats were daily weighed and their body condition was examined for health assessment. The variation of average body weight gain in rats of all groups either before or after AFB_1 intoxication showed no significance. Interestingly, the rats in AXH+AFB_1 group that have been gavaged by high dose AX for 7 days before AFB_1 administration gained less weight than others. However, the weight gain of rats in AFB_1 group became lowest after AFB_1 intoxication (Table 1).

Effect of AX and AFB_1 on liver weight (LW)

At 13th day, all rats were weighed and then euthanized to collect liver samples. An average body weight of rats in all groups showed no significant difference. However, the LW was significantly increased in AFB_1 group, while it was not different among control, AXL+AFB_1 and AXH+AFB_1 groups. The calculation of LW/100 g BW manifested significantly higher value in AFB_1 group when compared to control and both AX treated groups (Table 2).

Effects on liver function evaluated by serum ALT and AST levels

All experimental groups showed elevated serum ALT and AST as compared to control (Table 3). Especially, the level of serum ALT in AFB_1 group was significantly increased whereas this parameter revealed no significant difference from control in AXL+AFB_1 and AXH+AFB_1 groups. Nevertheless, average AST level of rats in control, AFB_1, AXL+AFB_1 and AXH+AFB_1 groups was not statistically different.

Liver histopathological findings

The histopathological changes of liver tissue occurred in all experimental groups apart from control rats, which revealed normal pattern of hepatic cord arrangement in hepatic lobules with intact portal areas (Fig. 1a). Besides normal hepatocytes, some megalocytic, binucleated and apoptotic hepatocytes were also presented in control group. The apoptotic cells were smaller than adjacent cells and showed hypereosinophilic cytoplasm from cytoplasmic condensation with pyknotic or fragmented nuclei [13] (Fig. 1b). After receiving 1 mg/kg AFB_1 for 4 days, massive vacuolar degeneration of hepatocytes were found in all hepatic lobules

Table 1. Average body weight gain before and after aflatoxin B_1 (AFB_1) intoxication

Group	Body weight gain (g)	
	Before AFB_1 (d1-d7)	After AFB_1 (d9-d13)
Control	50 ± 7.07	22 ± 11.51
AFB_1	38.75 ± 2.50	13.75 ± 4.79
AXL+AFB_1	37 ± 8.37	18.33 ± 10.41
AXH+AFB_1	33.33 ± 11.55	20 ± 14.14

Data is presented as mean ± SD. AXL: low dose astaxanthin, AXH: high dose astaxanthin.

Table 2. Average liver weight (LW), body weight (BW) and LW/100 g BW

Group	LW (g)	BW (g)	LW/100 g BW
Control	9.71 ± 0.14[a)]	242.50 ± 13.23	4 ± 0.24[a)]
AFB_1	11.50 ± 0.54[b)]	241.25 ± 20.97	4.83 ± 0.26[b)]
AXL+AFB_1	9.72 ± 0.70[a)]	225 ± 9.13	4.33 ± 0.28[a)]
AXH+AFB_1	9.74 ± 0.87[a)]	226.67 ± 15.28	4.27 ± 0.12[a)]

Data is presented as mean ± SD. a, b) indicate significant difference within a column (P<0.05). AFB_1: aflatoxin B_1, AXL: low dose astaxanthin, AXH: high dose astaxanthin.

Table 3. Serum alanine aminotransferase (ALT) and aspartate aminotransferase (AST) levels of experimental rats in each group

Group	ALT (U/*l*)	AST (U/*l*)
Control	24 ± 9.08[a)]	68.80 ± 29.23
AFB_1	57.67 ± 26.10[b)]	122.33 ± 33.50
AXL+AFB_1	25.67 ± 7.64[a)]	78 ± 28.69
AXH+AFB_1	42 ± 9.90[a)]	143.50 ± 54.45

Data is presented as mean ± SD. a, b) indicates significant difference within a column (P≤0.05). AFB_1: aflatoxin B_1, AXL: low dose astaxanthin, AXH: high dose astaxanthin.

of rats from AFB_1 group. Some hepatocytes underwent karyorrhexis and some degenerated cells exhibited really faint or nuclei absent (karyolysis) which indicated necrosis (Fig. 1c and 1d). Various degrees of typical bile duct hyperplasia and inflammatory cell infiltration were observed in all portal areas. Acidophilic megalocytes and binucleated hepatocytes were distributed in all lobules, though some of them had been degenerated (Fig. 1d). The rats in AXL+AFB_1 group gavaged by 5 mg/kg AX for 7 days before AFB_1 intoxication revealed different results compare with the AFB_1 treatment group. The vacuolar degenerative hepatocytes were found at periportal area, but were extended into midzonal to centrilobular areas in some lobules (Fig. 1e). The amount of megalocytes, binucleated cells and inflammatory cell infiltration were approximately equal to AFB_1 group (Fig. 1f), whereas bile duct hyperplasia was low. Noteworthy, one rat from this group showed distinct appearance of hypertrophic hepatocytes with extensive basophilic cholangiocyte proliferation. The vacuolar degenerative hepatocytes were rarely noticed in this rat. These hypertrophic cells were approximately two times larger in size when compared with normal hepatocyte, leading to disarrangement of hepatic cord. The sinusoids in these areas were narrowed. Some cells showed abnormal large sized nucleus and some were binucleated, but most cells possessed increasing cellular content but normal nuclear sizes with irregular cytoplasmic clumping below the plasma membrane and vesicular pattern of nuclei (Fig. 2). In AXH+AFB_1 group, one rat showed hepatic vacuolar degeneration and typical bile duct hyperplasia at periportal and midzonal areas with less severity than in AXL+AFB_1 group (Fig. 1g and 1h) but the others revealed predominant hypertrophic hepatocytes and cholangiocyte proliferation. Among these four rats in AXH+AFB_1 group, half of them showed slight hepatic vacuolar degeneration, but this occurrence was not existed within any lobules in another half. The mean value of all hepatocyte alterations in control group was the lowest except the number of apoptotic cells which was insignificantly higher than in AFB_1 and AXL+AFB_1 group. The degeneration and necrosis were remarkably high in AFB_1 group compared to other groups (P<0.05). Moreover, the AXL+AFB_1 group also showed significantly notable level of hepatocyte degeneration from AXH+AFB_1 group. The number of megalocyte was higher in AFB_1 and AXL+AFB_1 group than in AXH+AFB_1 group (P<0.05) while the binucleated cells in AFB_1 group was lower than in AXL+AFB_1 and AXH+AFB_1 groups (P<0.05). The AXH+AFB_1 group revealed low amount of necrotic cells which was not significantly different from control but the level was elevated in AXL+AFB_1 group (P<0.05). In contrast, the amount of apoptotic cells was high in AXH+AFB_1 group implying that the irreversibly degenerative cells in AXH+AFB_1 group were subjected to be eliminated by apoptosis instead of necrosis. The highest level of hypertrophic hepatocytes was also apparently observed in AXH+AFB_1 group though there was no significant difference among groups (Table 4).

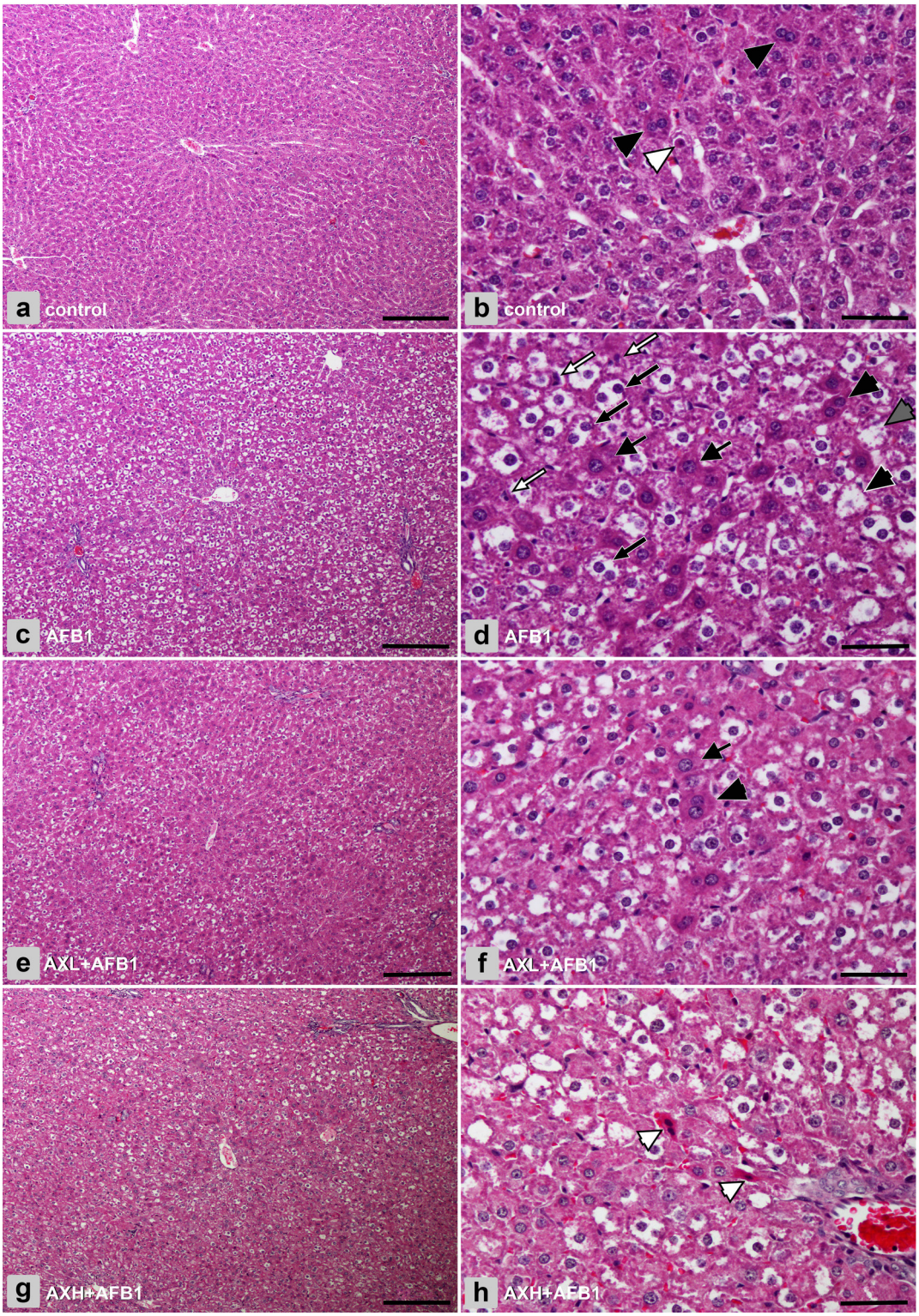

Fig. 1. The illustration of histopathological findings of rat liver in control group (a) showed normal histology which some megalocytes, binucleated hepatocytes and apoptotic cells could be noticed (b). Liver tissue from AFB_1 group (c) revealed massive vacuolar degeneration in all lobules and bile duct hyperplasia in portal area. Megalocytes, binucleated hepatocytes and their degenerated forms as well as necrotic cells that underwent karyorrhexis were extensively found in this group (d). The vacuolar degeneration of hepatocytes was gradually reduced from $AXL+AFB_1$ group to $AXH+AFB_1$ group (e and g). The appearance of megalocytes and binucleated cells was still high in $AXL+AFB_1$ group (f). Necrotic and apoptotic cells were slightly observed in $AXL+AFB_1$ and $AXH+AFB_1$ groups (h). Thick arrow; Megalocyte, Black arrowhead; Binucleated hepatocyte, Black thin arrow; Degenerative binucleated hepatocyte, White thin arrow; Necrotic cell (karyorrhexis), White arrowhead; Apoptotic cell. AFB_1: aflatoxin B_1, AXL: low dose astaxanthin, AXH: high dose astaxanthin. H&E. Bar in a, c, e, g=200 μm, Bar in b, d, f, h=50 μm.

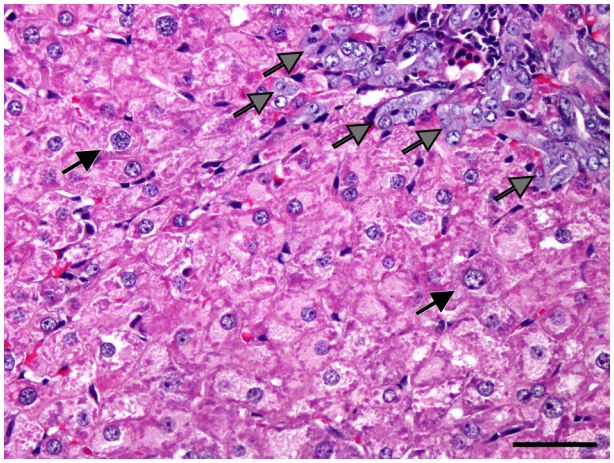

Fig. 2. Hypertrophic hepatocytes associated with proliferation of cholangiocytes (gray arrows) revealed in some rats of AXL+AFB_1 and AXH+AFB_1 groups (this picture is representative fom AXH+AFB_1 group). Few hepatocytes showed abnormal large sized nucleus (megalocytes; black arrows) but most cells possessed increasing cellular content but normal nuclear size. H&E. AXL: low dose astaxanthin, AXH: high dose astaxanthin, AFB_1: aflatoxin B_1. Bar=50 μm.

Table 4. Effects of aflatoxin B_1 (AFB_1) and astaxanthin on hepatocyte alterations

Group	Average cell number per square millimeter (cells/mm^2)					
	Vacuolar degenerative	Megalocytic	Binucleated	Necrotic	Apoptotic	Hypertrophic
Control	12.3 ± 15.9[a)]	7.9 ± 10.8[a)]	44.6 ± 30.6[a)]	2.0 ± 5.3[a)]	2.5 ± 5.0	0.0 ± 0.0
AFB_1	747.8 ± 229.7[b)]	54.6 ± 54.5[b)]	77.6 ± 31.2[b)]	117.8 ± 62.0[b)]	0.9 ± 3.3	0.9 ± 3.3
AXL+AFB_1	488.4 ± 330.4[c)]	48.5 ± 31.4[b)]	93.9 ± 39.2[c)]	42.2 ± 35.6[c)]	1.8 ± 7.2	2.0 ± 7.2
AXH+AFB_1	47.7 ± 42.9[d)]	26.2 ± 19.8[c)]	91.8 ± 36.9[c)]	5.2 ± 7.7[a)]	3.2 ± 6.2	32.5 ± 26.8

Data is presented as mean ± SD. a–d) indicates significant difference within a column (P<0.05). AXL: low dose astaxanthin, AXH: high dose astaxanthin.

Immunohistochemistry and expression of SOD1

The SOD1 immunostaining of liver cells in control group revealed of dark brown color either in cytoplasm or nuclei (Fig. 3a) whereas degenerative cells in AFB_1 group were stained only at nuclei and edge of cells and the necrotic cells were unstained. Very few cells were fully stained in the cytoplasm (Fig. 3b). For AXL+AFB_1 group, the hepatocytes displayed variety of immunoreactivity but mostly were illustrated as moderate brown staining (Fig. 3c). The higher immunostaining was seen in hepatocytes of AXH+AFB_1 group, which were filled by visible dark brown color (Fig. 3d). The percentage of brown staining area from each group was quantified to indicate differences of SOD1 expression level. The SOD1 immunostaining from control, AFB_1, AXL+AFB_1 and AXH+AFB_1 groups was shown as 37.61, 31.47, 33.16 and 35.43%, respectively. The analysis of these measurement implied that SOD1 expression in hepatocytes of AXH+AFB_1 group was significantly elevated comparing to AFB_1 and AXL+AFB_1 groups. Control group significantly presented the highest level of SOD1 immunostaining whereas the percentage of staining area between AFB_1 and AXL+AFB_1 groups was not significantly different (Fig. 4). The western blot analysis was performed in order to confirm whether AX could induce expression of SOD1 in AFB_1 ingested rat as shown in immunohistochemistry. The result manifested that SOD1 expression was slightly increased in AXH+AFB_1 group from the control but markedly declined in AFB_1 group (P<0.05). However, the expression level of SOD1 was not much different between AFB_1 and AXL+AFB_1 groups (Fig. 5).

DISCUSSION

Although the body weight gain in all groups was not significantly different during the first week of experimental period, the declined weigh and food intake of rats in AXH+AFB_1 group has been noticed. No sign of illness was examined in these rats. Since the AX used in this experiment is a feed additive grade for aquatic animals, it was 10% mixture with calcium lignosulfonate to facilitate the administration into water-based foods. We speculate that highly viscous ingredients might completely fill in rat stomach and alleviate appetite. Indeed, an overdose of vitamin A has been known to induce appetite loss and growth reduction [24], but an AX dosage of 100 mg/kg has been orally administered in rats for 15 days without any adverse effect [20]. Therefore, the dosage used in this study might not high enough to promote toxicity. After AFB_1 gavage, the difference of body weight gain

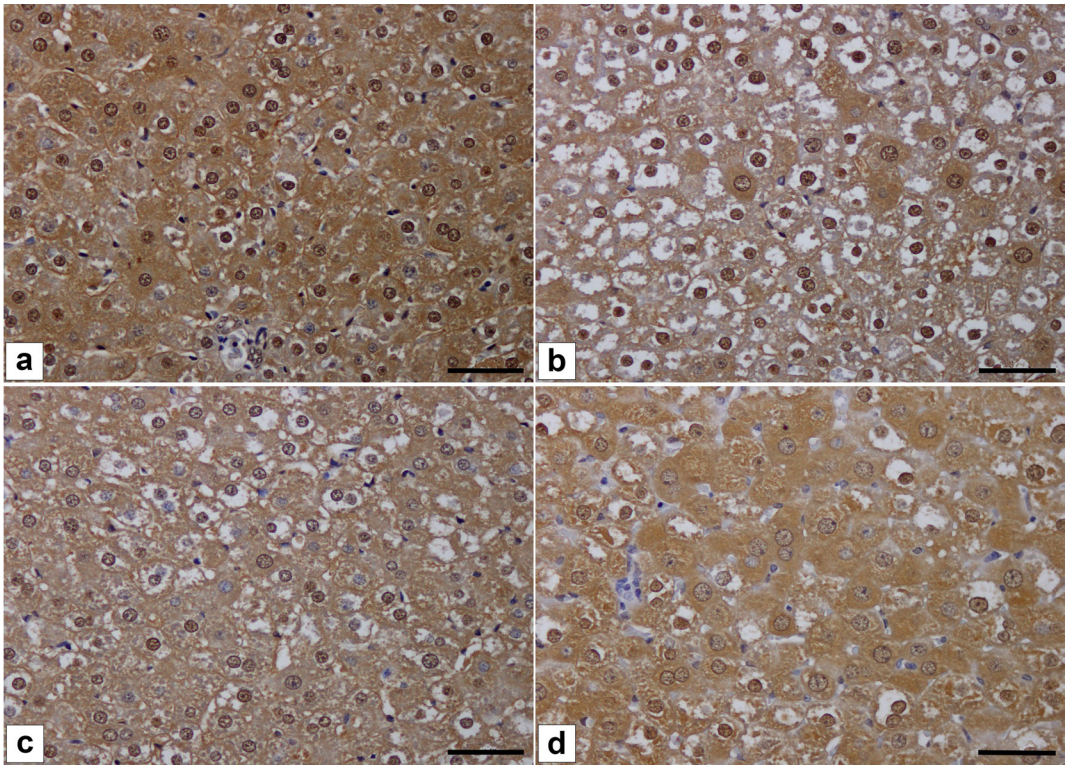

Fig. 3. Superoxide dismutase 1 (Cu/Zn-SOD: SOD1) Immunoreactivity demonstrated an expression in hepatocytes of (a) control, (b) AFB_1, (c) $AXL+AFB_1$ and (d) $AXH+AFB_1$ groups. The other types of cell, such as Kupffer cells and endothelial cells, were stained blue from hematoxylin dye. AFB_1: aflatoxin B_1, AXL: low dose astaxanthin, AXH: high dose astaxanthin. Bar=50 μm.

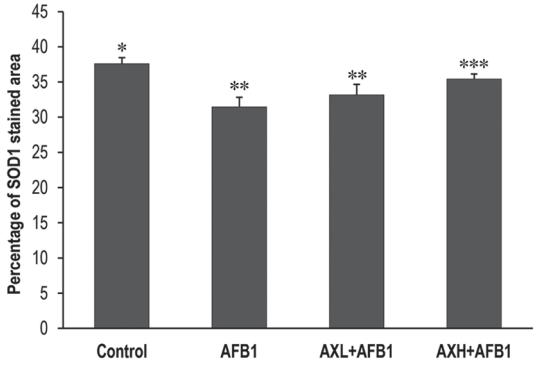

Fig. 4. Percentage of superoxide dismutase 1 (Cu/Zn-SOD: SOD1) immunostained area from control, AFB_1, $AXL+AFB_1$ and $AXH+AFB_1$ groups. AFB_1: aflatoxin B_1, AXL: low dose astaxanthin, AXH: high dose astaxanthin. *,**,*** indicate significant difference among groups.

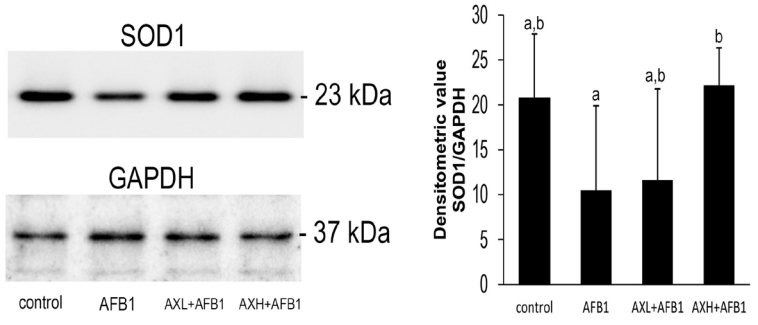

Fig. 5. Western blot analysis of liver extract containing 25 μg of protein in each lane to detect superoxide dismutase 1 (Cu/Zn-SOD: SOD1) and Glyceraldehyde-3-phosphate dehydrogenase (GAPDH) band density. Normalized densitometric values of SOD1/GAPDH, presented as mean ± SD, indicated that the SOD1 expression level in $AXH+AFB_1$ group was significantly higher than that in AFB_1 group ($P<0.05$). AFB_1: aflatoxin B_1, AXL: low dose astaxanthin, AXH: high dose astaxanthin. a and b indicate significant difference among groups.

between groups was also insignificant. Nevertheless, an average weight gain of rats from AFB_1 group was obviously less than others, whereas the $AXH+AFB_1$ group was elevated. Qian *et al.* (2013) showed similar result in the toxicological study of AFB_1 exposure in rats, but the body weight gain of 1 mg/kg AFB_1 exposed rats was significantly decreased when compared to the control [34]. This result implies that AX could help to enhance body weight in rats receiving AFB_1.

An average LW and LW / 100 g BW of rats in AFB_1 group was significantly higher than other groups, while those of rats in control, $AXL+AFB_1$ and $AXH+AFB_1$ groups showed little difference. From our study, the acute intoxication of high dose AFB_1

recruited inflammatory response in liver tissue which was shown as inflammatory cells infiltration around portal areas. This occurrence was also consistent with reports of some studies indicating that an increased liver weight was subsequently a result from massive liver inflammation [20, 34]. Noteworthy, the insignificant difference of average LW and LW / 100 g BW between control and both of AX treated groups implies that AX possessed an anti-inflammatory potential in rat liver towards acute AFB_1 intoxication. Previous studies revealed that AX reduces pro-inflammatory cytokines which cause liver damage by a toxic dose of acetaminophen, such as TNF-α and IL-6, within 24 hr [50]. Beside the inhibition of acute inflammation, AX also inhibits chronic inflammation which could induce hepatic fibrosis by decreasing of TGF-β1 expression via down regulation of NF-κB [22, 39].

AX could restore liver function from AFB_1 induced destruction as inspected by the significantly declining level of ALT in rats received AX for 1 week before AFB_1 intoxication (Table 3). The AST level, despite no statistically significant difference among groups, the level in AXH+AFB_1 group was only slightly different from AFB_1 group, whereas this enzyme in AXL+AFB_1 group had almost similar level to control group. It is surprising that an equal dosage of AX used significantly reduced serum ALT and AST levels in CCl_4 induced rats [20], although we gave half shorter duration of AX treatment before inducing hepatocellular damage by AFB_1. We also suspect whether calcium lignosulfonate might have hepatotoxic action since its high concentration has been mixed with AX and gavaged into rats in this group. However, this hypothesis might be untrue because this polymer of lignin is considered safe as a feed additive in animals [12]. As a result of its high molecular weight, calcium lignosulfonate is poorly absorbed from the gastrointestinal tract of rats. In addition, the *in vitro* studies also show low transepithelial transport in Caco2 cells. Therefore, the presence of substantial amount of this compound in the tissues is unlikely [11]. Furthermore, the JECFA set an acceptable daily intake of calcium lignosulfonate, based on a 90-day rat study, at a dosage up to 2,000 mg/kg body weight [19, 42]. Accordingly, such amount of calcium lignosulfonate given to rats in AXH+AFB_1 group is not possible to cause hepatotoxic. Moreover, it was also confirmed that the causation of the lowest weight gain of rats in AXH+AFB_1 group in the first period of our experiment was from an indigestible calcium lignosulfonate as described above.

The AFB_1 is known to have hepatotoxic potency. In this study, massive degeneration, necrosis, magalocytosis, and binucleation of hepatocytes were induced in the liver of rats administered a high single dose of AFB_1 (Fig. 1c and 1d). These incidences were found throughout the hepatic lobules but mostly localized at periportal to midzonal areas. The finding is similar to a report of Qian *et al.* (2013) [34] but contrast to the chronic intoxication by repeating low dosage of AFB_1 which hydropic degeneration was primarily detected at centrilobular (periacinar) and midzonal regions of hepatic lobules [48]. The hepatocytes residing around centrilobular area own the highest concentration of microsomal cytochrome P450 which activates AFB_1 metabolism to produce a highly reactive intermediate, the 8, 9-epoxide metabolite [10, 41]. Therefore, the centrilobular hepatocytes tend to be more sensitive to AFB_1 induced liver damage than the periportal ones. Nevertheless, the AFB_1 from intestinal absorption is circulated in portal vein located in portal area before distributing toward the centrilobular region. We speculate that, after oral administration with high dose AFB_1, the amount of AFB_1 predominantly concentrated and metabolized in periportal and midzonal hepatocytes was high enough to immediately degenerate and destroy cells. Thus, the vacuolar degeneration and necrosis of hepatocytes were mainly focused in these areas instead of centrilobular region. The ROS produced from AFB_1 metabolism affect cell membrane integrity leading to calcium influx and cell swelling as the initial process of vacuolar degeneration [8]. This pathological change was declined in AXL+AFB_1 group (Fig. 1e and 1f) and obviously reduced in AXH+AFB_1 group (Fig. 1g and 1h) indicating the protective effects of AX to the cell from degenerative process. The damage of cell membrane is primarily activated by peroxyl radical generated in the process of lipid peroxidation, and carotenoids are known the efficient scavenger for this ROS [31]. Therefore, AX should certainly have scavenging efficacy against peroxyl radical as in other carotenoids. Besides cellular degeneration and necrosis, megalocytosis and binucleation of hepatocytes were also noted in all groups especially in AFB_1 administered groups. Since aflatoxin has antimitotic effect, though less capable than pyrrolizidine alkaloid, the replacement of AFB_1 damaged hepatocytes by naturally proliferation is limited, especially in the prolonged aflatoxicosis [10, 30]. As a result, the cellular and nuclear enlargement of cell displaying active DNA and protein synthesis but impaired cell division is occurred, so called megalocytosis [3]. However, the feasibility of megalocyte as a precancerous cell is not confirmed although the study of liver carcinogenesis in Wistar rats with a single dose of 7 mg/kg AFB_1 or subsequently repeated CCl_4 inhalation demonstrates that megalocytosis is the first observed lesion and the tumor cells usually located among the megalocytic cells [38]. In another aspect, polyploidy, which is usually found as megalocyte and binucleated cell, could also denote an adaptive mechanism to become more resistant to oxidative stress and genotoxic damage from xenobiotic [4, 14, 17, 28]. Several researchers elucidated that diploid hepatocytes enter the cell cycle faster than polyploid cells. Moreover, multiple copies of tumor suppressors in polyploid hepatocytes reduce the likelihood of transformation, whereas diploid hepatocytes have only two copies and are prone to tumorigenesis by inactivating mutation of these genes. These advantages of polyploidy eventually reduce the expansion of transformed genes into the progeny [14, 46]. According to our result, we hypothesized that increased megalocyte in AFB_1 ingested rat was due to dual causation, AFB_1 toxicity and adaptation to toxin. AX treated groups exhibited less number of megalocyte than in AFB_1 group because it could alleviate AFB_1 toxicity. Meanwhile, the adaptive response in AX treated groups shown as polyploidy led to higher number of binucleated hepatocyte (Table 4).

The bile duct hyperplasia exhibited in AFB_1 group was a typical proliferation of cholangiocytes which demonstrated as newly formed bile ducts with well-defined lumens [23]. This is relevant to an observation from Qian *et al.* (2013) in rats orally administered by 1 mg/kg AFB_1 [34]. In AXL+AFB_1 group, most rats also showed similar morphology of bile duct hyperplasia, except one rat that revealed cholangiocyte proliferation originated at portal area and extended into surrounding hepatic parenchyma coincided with hypertrophy of hepatocytes (Fig. 2). The same incidence was also noted in most rats from AXH+AFB_1 group. This atypical cholangiocyte proliferation was supposed to be a ductular reaction to restore the nearby damaged hepatocytes during

liver injury. The regeneration is arisen from transdifferentiation of proliferated cholangiocytes into hepatocytes [37]. In acute liver injury, destroyed hepatocytes are replaced by β-catenin dependent proliferation of neighboring alive hepatocytes. However, the β-catenin dependent regenerative response is impaired in case of severe or chronic injury. Thus, the hepatocyte repopulation will be relied on β-catenin independent cholangiocyte-to-hepatocyte differentiation that will be occurred after damaging causes have been eradicated [32]. AX is well documented for its anti-oxidative activity. The elimination of free radicals and ROS generated from AFB_1 metabolism is considered to remove cause of liver damage, leading to improvement of liver tissue by atypical cholangiocytes proliferation, as seen in some rats from AXL+AFB_1 and AXH+AFB_1 groups. Ultimately, these cells will be derived into hepatocytes. Moreover, the hepatocytes predominantly found in these rats showed the morphology of hypertrophy with cytoplasmic clumping and vesicular nucleus. According to a review of Hall *et al*. (2012), an increased size of liver cell could be resulted from elevated protein production and proliferation of subcellular organelles typically sER and/or peroxisome. From the experiment of microsomal enzymes inducer administration in rats, the hypertrophy of hepatocytes was examined through smooth ER proliferation observed by electron microscopic study which demonstrated characteristic stacks of smooth ER that crowd out other organelles. Some xenobiotics also induce peroxisome proliferation which presented as catalase positive electron dense vesicles in the cytoplasm. Importantly, both circumstances are considered adaptive and non-adverse responses to induce hepatic metabolism. However, these responses can be failed at higher dose levels or following prolonged exposure, if degenerative changes of hepatocytes are overcome or novel cytotoxic metabolites are generated [16]. These data supports our observations, especially in AXH+AFB_1 group, revealing hepatocyte hypertrophy which was suspected to contain cytoplasmic proteins with accumulation of multiplied organelles involving production of those anti-oxidative enzymes (Table 4). Moreover, the higher serum ALT level, but not above two times than control, in AXH+AFB_1 group might indicate a consequence of increased enzyme synthesis, as also noted by Hall *et al*. (2012) [16].

In the liver, the AFB_1 toxicity through AFB_1-8, 9-epoxide causes generation of intracellular ROS leading to oxidative stress and damage of vital components such as DNA and cell membrane [21, 25, 27]. The cellular anti-oxidative activities are deprived in 1 mg/kg AFB_1 administered rats as shown by increasing lipid peroxidation and decreased various anti-oxidative enzymes, such as SOD, CAT, GPX and glutathione-S-transferase [33]. SOD has been shown to have a protective effect on liver injury induced by AFB_1 [20, 27, 40, 48, 49]. It is responsible for the first line of antioxidant defensive system against cell injury from the highly ROS generated by biochemical redox reactions in normal cell metabolism, and by exogenous sources. The SOD1 expression is stronger in normal liver tissue comparing to hepatocellular carcinoma in the same patient. However, superoxide radicals and other ROS generated in malignant cells are probably diffuse into surrounding tissue and further damaging it. The up-regulation of SOD and other antioxidative enzymes is likely the mechanism to resist the damage from increasing oxidative stress in hepatocyte [45]. SOD1 is ascribed to be synthesized by ribosomes. Its distribution in the cytosol is unsuspicious but the existence in nuclear matrix is believed to occur by diffusion of cytosolic SOD1 into the nucleus through nuclear pores [6]. The localization of SOD1 is corresponding to the finding from our present study. Additionally, our study obviously revealed the SOD1 expression decreased in the liver of rats in AFB_1 group, whereas the expression of this enzyme in AXH + AFB_1 group was significantly higher (Figs. 4 and 5). This result implies that AX potentially induces SOD1 expression as same as in previous reports [5, 20]. The similar result has been demonstrated in a study of curcumin hepatoprotective effects against aflatoxicosis. It was also found that curcumin stimulates up-regulation of anti-oxidative enzyme gene expression such as SOD and GPX. Additionally, curcumin also demonstrates other anti-oxidative activities by scavenging ROS through interaction within the oxidative cascade and inhibiting aflatoxin biotransformation by restriction of cytochrome P450, thus decreasing the formation of AFB_1-8, 9-epoxide [27]. Though we did not intensively study for anti-oxidative effects of AX as in curcumin, the existing results are substantial to conclude that AX possesses hepatoprotective role in rat aflatoxicosis. The AFB_1 generated ROS that consequently damaged hepatocytes as shown by elevated liver enzyme parameters and histopathological changes of vacuolar degeneration and cell necrosis. AX could alleviate cellular damage by diminishing degenerative and necrotic changes as well as serum ALT level in AXL+AFB_1 and AXH+AFB_1 groups. Some rats from AX treated groups also exhibited atypical proliferation of cholangiocytes which is believed to be a process of transdifferentiation to replace damaged hepatocytes. Likewise, both AX treated groups demonstrated higher percentage of SOD1 stained area when compared to AFB_1 group. This result also corresponds to the western blot analysis indicating that SOD1 expression was induced by AX. However, the values in AXL+AFB_1 group were not significantly different from AFB_1 group, denoting that the AX induced SOD1 expression was dose dependent. The level of SOD1 expression in AXH+AFB_1 group that was above the control could also verify increased activity of SOD1 production. Additionally, the hypertrophy of hepatocytes mostly found in rats receiving 100 mg/kg AX prior to AFB_1 administration in AXH+AFB_1 group may imply the over production of detoxifying proteins and accumulation of involving cytoplasmic organelles to mitigate AFB_1 toxicity.

ACKNOWLEDGMENTS. This research was supported by the Faculty of Veterinary Medicine, Kasetsart University. The authors thank Department of Zoology, Faculty of Science, Kasetsart University for facilitating animal laboratory. Special thanks to Associated Professor Chaiyan Kasorndorkbua, Department of Pathology, Faculty of Veterinary Medicine, Kasetsart University, for his helpful guidance in histopathology of AFB_1 toxicity in rat liver.

REFERENCES

1. Abdel-Latif, M. S., Elmeleigy, K. M., Aly, T. A. A., Khattab, M. S. and Mohamed, S. M. 2017. Pathological and biochemical evaluation of coumarin and chlorophyllin against aflatoxicosis in rat. *Exp. Toxicol. Pathol.* **69**: 285–291. [Medline] [CrossRef]

2. Basappa, S. C. 2009. Aflatoxins, Formation, Analysis and Control. Alpha Science International Ltd., Oxford.
3. Bischoff, K., Mukai, M. and Ramaiah, S. K. 2018. Liver toxicity. pp. 239–258. *In*: Veterinary Toxicology: Basic and Clinical Principles, 3rd ed. (Gupta, R. C. ed.), Elsevier, London.
4. Bortolin, J. A., Quintana, H. T., Tomé, T. C., Ribeiro, F. A. P., Ribeiro, D. A. and de Oliveira, F. 2016. Burn injury induces histopathological changes and cell proliferation in liver of rats. *World J. Hepatol.* **8**: 322–330. [Medline] [CrossRef]
5. Cao, J. and Wang, W. 2014. Effect of astaxanthin and esterified glucomannan on hematological changes in broilers fed aflatoxin-B1-contaminated feed. *Anim. Sci. J.* **85**: 150–157. [Medline] [CrossRef]
6. Chang, L. Y., Slot, J. W., Geuze, H. J. and Crapo, J. D. 1988. Molecular immunocytochemistry of the CuZn superoxide dismutase in rat hepatocytes. *J. Cell Biol.* **107**: 2169–2179. [Medline] [CrossRef]
7. Choi, S. K., Kim, J. H., Park, Y. S., Kim, Y. J. and Chang, H. I. 2007. An efficient method for the extraction of astaxanthin from the red yeast *Xanthophyllomyces dendrorhous*. *J. Microbiol. Biotechnol.* **17**: 847–852. [Medline]
8. Cotran, R. S., Kumar, V. and Collins, T. 1999. Robbins Pathologic Basis of Disease, 6th ed., W. B. Saunders Company, Philadelphia.
9. Crapo, J. D., Oury, T., Rabouille, C., Slot, J. W. and Chang, L. Y. 1992. Copper,zinc superoxide dismutase is primarily a cytosolic protein in human cells. *Proc. Natl. Acad. Sci. U.S.A.* **89**: 10405–10409. [Medline] [CrossRef]
10. Cullen, J. M. and Stalker, M. J. 2016. Liver and biliary system. pp. 258–352. *In*: Jubb, Kennedy, and Palmer's Pathology of Domestic Animals (Volume 2), 6th ed. (Maxie, M. G. ed.), Elsevier, St. Louis.
11. EFSA ANS Panel (EFSA Panel of Food Additives and Nutrient Sources Added to Food) 2010. Scientific opinion on the use of calcium lignosulfonate (40–65) as a carrier for vitamins and carotenoids. *EFSA J.* **8**: 1525.
12. EFSA FEEDAP Panel (EFSA Panel on Additives and Products or Substances used in Animal Feed) 2015. Scientific opinion on the safety and efficacy of lignosulphonate as a feed additive for all animal species. *EFSA J.* **13**: 4160.
13. Elmore, S. A., Dixon, D., Hailey, J. R., Harada, T., Herbert, R. A., Maronpot, R. R., Nolte, T., Rehg, J. E., Rittinghausen, S., Rosol, T. J., Satoh, H., Vidal, J. D., Willard-Mack, C. L. and Creasy, D. M. 2016. Recommendations from the INHAND apoptosis/ necrosis working group. *Toxicol. Pathol.* **44**: 173–188. [Medline] [CrossRef]
14. Gentric, G. and Desdouets, C. 2014. Polyploidization in liver tissue. *Am. J. Pathol.* **184**: 322–331. [Medline] [CrossRef]
15. Ha, H. L., Shin, H. J., Feitelson, M. A. and Yu, D. Y. 2010. Oxidative stress and antioxidants in hepatic pathogenesis. *World J. Gastroenterol.* **16**: 6035–6043. [Medline] [CrossRef]
16. Hall, A. P., Elcombe, C. R., Foster, J. R., Harada, T., Kaufmann, W., Knippel, A., Küttler, K., Malarkey, D. E., Maronpot, R. R., Nishikawa, A., Nolte, T., Schulte, A., Strauss, V. and York, M. J. 2012. Liver hypertrophy: a review of adaptive (adverse and non-adverse) changes—conclusions from the 3rd International ESTP Expert Workshop. *Toxicol. Pathol.* **40**: 971–994. [Medline] [CrossRef]
17. Hsu, S. H. and Duncan, A. W. 2015. Pathological polyploidy in liver disease. *Hepatology* **62**: 968–970. [Medline] [CrossRef]
18. Ismail, A., Gonçalves, B. L., de Neeff, D. V., Ponzilacqua, B., Coppa, C. F. S. C., Hintzsche, H., Sajid, M., Cruz, A. G., Corassin, C. H. and Oliveira, C. A. F. 2018. Aflatoxin in foodstuffs: Occurrence and recent advances in decontamination. *Food Res. Int.* **113**: 74–85. [Medline] [CrossRef]
19. JECFA (Joint FAO/WHO Expert Committee on Food Additives) 2009. Safety evaluation of certain food additives. *WHO Food Addit. Ser.* **60**: http://www.inchem.org/documents/jecfa/jecmono/v60je01.pdf [accessed on October 1, 2018].
20. Kang, J. O., Kim, S. J. and Kim, H. 2001. Effect of astaxanthin on the hepatotoxicity, lipid peroxidation and antioxidative enzymes in the liver of CCl_4-treated rats. *Methods Find. Exp. Clin. Pharmacol.* **23**: 79–84. [Medline] [CrossRef]
21. Klaunig, J. E., Wang, Z., Pu, X. and Zhou, S. 2011. Oxidative stress and oxidative damage in chemical carcinogenesis. *Toxicol. Appl. Pharmacol.* **254**: 86–99. [Medline] [CrossRef]
22. Lee, S. J., Bai, S. K., Lee, K. S., Namkoong, S., Na, H. J., Ha, K. S., Han, J. A., Yim, S. V., Chang, K., Kwon, Y. G., Lee, S. K. and Kim, Y. M. 2003. Astaxanthin inhibits nitric oxide production and inflammatory gene expression by suppressing I(κ)B kinase-dependent NF-kappaB activation. *Mol. Cells* **16**: 97–105. [Medline]
23. LeSage, G., Glaser, S. and Alpini, G. 2001. Regulation of cholangiocyte proliferation. *Liver* **21**: 73–80. [Medline] [CrossRef]
24. Lind, T., Lind, P. M., Hu, L. and Melhus, H. 2018. Studies of indirect and direct effects of hypervitaminosis A on rat bone by comparing free access to food and pair-feeding. *Ups. J. Med. Sci.* **123**: 82–85. [Medline] [CrossRef]
25. McCord, J. M. 2000. The evolution of free radicals and oxidative stress. *Am. J. Med.* **108**: 652–659. [Medline] [CrossRef]
26. Miki, W. 1991. Biological functions and activities of animal carotenoids. *Pure Appl. Chem.* **63**: 141–146. [CrossRef]
27. Mohajeri, M., Behnam, B., Cicero, A. F. G. and Sahebkar, A. 2018. Protective effects of curcumin against aflatoxicosis: A comprehensive review. *J. Cell. Physiol.* **233**: 3552–3577. [Medline] [CrossRef]
28. Monga, S. P. S. 2014. Hepatic regenerative medicine: exploiting the liver's will to live. *Am. J. Pathol.* **184**: 306–308. [Medline] [CrossRef]
29. Naguib, Y. M. 2000. Antioxidant activities of astaxanthin and related carotenoids. *J. Agric. Food Chem.* **48**: 1150–1154. [Medline] [CrossRef]
30. Neal, G. E., Judah, D. J. and Butler, W. H. 1976. Some effects of acute and chronic dosing with aflatoxin B_1 on rat liver nuclei. *Cancer Res.* **36**: 1771–1778. [Medline]
31. Nimse, S. B. and Pal, D. 2015. Free radicals, natural antioxidants, and their reaction mechanisms. *RSC Advances* **5**: 27986–28006. [CrossRef]
32. Perugorria, M. J., Olaizola, P. and Banales, J. M. 2018. Cholangiocyte-to-hepatocyte differentiation: a context dependent process and an opportunity for regenerative medicine. *Hepatology* 10.1002/hep.30305. [Medline]
33. Preetha, S. P., Kanniappan, M., Selvakumar, E., Nagaraj, M. and Varalakshmi, P. 2006. Lupeol ameliorates aflatoxin B1-induced peroxidative hepatic damage in rats. *Comp. Biochem. Physiol. C Toxicol. Pharmacol.* **143**: 333–339. [Medline] [CrossRef]
34. Qian, G., Wang, F., Tang, L., Massey, M. E., Mitchell, N. J., Su, J., Williams, J. H., Phillips, T. D. and Wang, J. S. 2013. Integrative toxicopathological evaluation of aflatoxin B_1 exposure in F344 rats. *Toxicol. Pathol.* **41**: 1093–1105. [Medline] [CrossRef]
35. Rahman, M. M., Khosravi, S., Chang, K. H. and Lee, S. M. 2016. Effects of dietary inclusion of astaxanthin on growth, muscle pigmentation and antioxidant capacity of juvenile rainbow trout (*Oncorhynchus mykiss*). *Prev. Nutr. Food Sci.* **21**: 281–288. [Medline] [CrossRef]
36. Ranga, R., Sarada, A. R., Baskaran, V. and Ravishankar, G. A. 2009. Identification of carotenoids from green alga *Haematococcus pluvialis* by HPLC and LC-MS (APCI) and their antioxidant properties. *J. Microbiol. Biotechnol.* **19**: 1333–1341. [Medline]
37. Sato, K., Marzioni, M., Meng, F., Francis, H., Glaser, S. and Alpini, G. 2018. Ductular reaction in liver diseases: pathological mechanisms and translational significances. *Hepatology* 10.1002/hep.30150. [Medline]
38. Scotto, J. M., Stralin, H. G., Lageron, A. and Lemonnier, F. J. 1975. Influence of carbon tetrachloride or riboflavin on liver carcinogenesis with a single dose of aflatoxin b1. *Br. J. Exp. Pathol.* **56**: 133–138. [Medline]
39. Shen, M., Chen, K., Lu, J., Cheng, P., Xu, L., Dai, W., Wang, F., He, L., Zhang, Y., Chengfen, W., Li, J., Yang, J., Zhu, R., Zhang, H., Zheng, Y., Zhou, Y. and Guo, C. 2014. Protective effect of astaxanthin on liver fibrosis through modulation of TGF-β1 expression and autophagy. *Mediators*

Inflamm. **2014**: 954502. [Medline] [CrossRef]
40. Singh, K. B., Maurya, B. K. and Trigun, S. K. 2015. Activation of oxidative stress and inflammatory factors could account for histopathological progression of aflatoxin-B1 induced hepatocarcinogenesis in rat. *Mol. Cell. Biochem.* **401**: 185–196. [Medline] [CrossRef]
41. Smela, M. E., Currier, S. S., Bailey, E. A. and Essigmann, J. M. 2001. The chemistry and biology of aflatoxin B_1: from mutational spectrometry to carcinogenesis. *Carcinogenesis* **22**: 535–545. [Medline] [CrossRef]
42. Thiel, A., Braun, W., Cary, M. G., Engelhardt, J. A., Goodman, D. G., Hall, W. C., Romeike, A. and Ward, J. M. 2013. Calcium lignosulphonate: re-evaluation of relevant endpoints to re-confirm validity and NOAEL of a 90-day feeding study in rats. *Regul. Toxicol. Pharmacol.* **66**: 286–299. [Medline] [CrossRef]
43. Toyes-Vargas, E., Ortega-Pérez, R., Espinoza-Villavicencio, J. L., Arellano-Pérez, M., Civera, R. and Palacios, E. 2018. Effect of marine by-product meals on hen egg production parameters, yolk lipid composition and sensory quality. *J. Anim. Physiol. Anim. Nutr. (Berl.)* **102**: 462–473. [Medline] [CrossRef]
44. Tulayakul, P., Dong, K. S., Li, J. Y., Manabe, N. and Kumagai, S. 2007. The effect of feeding piglets with the diet containing green tea extracts or coumarin on *in vitro* metabolism of aflatoxin B1 by their tissues. *Toxicon* **50**: 339–348. [Medline] [CrossRef]
45. Vlaykova, T., Gulubova, M., Vlaykova, D., Cirovski, G., Yovchev, Y. and Julianov, A. 2008. Expression of the xenobiotic- and reactive oxygen species−detoxifying enzymes, GST-Pi, Cu/Zn-SOD and Mn-SOD in primary hepatocellular carcinoma. *TJS* **6**: 14–21.
46. Wilkinson, P. D., Delgado, E. R., Alencastro, F., Leek, M. P., Roy, N., Weirich, M. P., Stahl, E. C., Otero, P. A., Chen, M. I., Brown, W. K. and Duncan, A. W. 2019. The polyploid state restricts hepatocyte proliferation and liver regeneration in mice. *Hepatology* **69**: 1242–1258. [Medline] [CrossRef]
47. Williams, J. H., Phillips, T. D., Jolly, P. E., Stiles, J. K., Jolly, C. M. and Aggarwal, D. 2004. Human aflatoxicosis in developing countries: a review of toxicology, exposure, potential health consequences, and interventions. *Am. J. Clin. Nutr.* **80**: 1106–1122. [Medline] [CrossRef]
48. Yaman, T., Yener, Z. and Celik, I. 2016. Histopathological and biochemical investigations of protective role of honey in rats with experimental aflatoxicosis. *BMC Complement. Altern. Med.* **16**: 232–242. [Medline] [CrossRef]
49. Yener, Z., Celik, I., Ilhan, F. and Bal, R. 2009. Effects of *Urtica dioica* L. seed on lipid peroxidation, antioxidants and liver pathology in aflatoxin-induced tissue injury in rats. *Food Chem. Toxicol.* **47**: 418–424. [Medline] [CrossRef]
50. Zhang, J., Zhang, S., Bi, J., Gu, J., Deng, Y. and Liu, C. 2017. Astaxanthin pretreatment attenuates acetaminophen-induced liver injury in mice. *Int. Immunopharmacol.* **45**: 26–33. [Medline] [CrossRef]